

The Virulence Index: A Metric for Quantitative Analysis of Phage Virulence

Zachary J. Storms, PhD, Matthew R. Teel, Kevin Mercurio, and Dominic Sauvageau, PhD

Abstract

Background: One of the main challenges in developing phage therapy and manufacturing phage products is the reliable evaluation of their efficacy, performance, and quality. Since phage virulence is intrinsically difficult to fully capture, researchers have turned to rapid but partially inadequate methods for its evaluation.

Materials and Methods: This study demonstrates a standardized quantitative method to assess phage virulence based on three parameters: the virulence index (V_P)—quantifying the virulence of a phage against a host, the local virulence (v_i)—assessing killing potential at given multiplicities of infection (MOIs), and MV_{50} —the MOI at which the phage achieves 50% of its maximum theoretical virulence. This was shown through comparative analysis of the virulence of phages T4, T5, and T7.

Results: Under the conditions tested, phage T7 displayed the highest virulence, followed by phage T4 and, finally, by phage T5. The impact of parameters such as temperature and medium composition on virulence was shown for each phage. The use of the method to evaluate the virulence of combinations of phages—for example, for cocktail formulation—is also shown with phages T5 and T7.

Conclusions: The method presented provides a platform for high-throughput quantitative assessment of phage virulence and quality control of phage products. It can also be applied to phage screening, evaluation of phage strains, phage mutants, infection conditions and/or the susceptibility of host strains, and the formulation of phage cocktails.

Keywords: bacteriophage infection, bacterial reduction curve, comparative virulence, virulence quantification, quality control, high-throughput analysis

Introduction

DESPITE THE SIGNIFICANT IMPACT bacteriophages (phages) have had in understanding genetics and gene regulation,¹ and the enormous estimated number of phages present on this planet,² a relatively small number of phage species have been identified, and fewer have been fully characterized. But this is rapidly changing. Initiatives have been launched to both isolate new phage species and annotate the staggering amount of genomic data collected in the growing number of screening and characterization studies (the PhAnToMe project, the Marine Phage Sequencing project, and the SEA-PHAGE project^{3–5} are just some examples). There are also numerous ongoing efforts to identify phages suitable for phage therapy,^{6–9} biocontrol,^{10,11} prevention of biofilms,^{12,13} detection and diagnostics,^{14–16} and as active or structural elements in biomaterials.^{17,18}

With the rapidly growing number of applications comes an increasing need for the manufacture of phages and phage products, and by extension for approaches and methods to reliably assess their efficacy and quality. And considering that

phages are dynamic by nature—be it through mutations^{19–23} or phenotypic traits^{23–26}—the assessment of their efficacy cannot solely be based on approaches used for most other biologics—for example, peptides, proteins, or even monoclonal antibodies.

Phage infections depend on many factors—some correlated, others orthogonal—that affect infection dynamics and efficacy of phage products. The evaluation of how single parameters (titer, burst size, efficacy of plating, eclipse time, lysis time, etc.)^{20,27,28} affect a crucial factor such as virulence—that is, the killing ability of the phage—is not sufficient since these all contribute together to phage virulence. In fact, there is no current way of relating these parameters or weighing their individual or combined input toward the overall phage virulence. Hence, the characterization of phages, the evaluation of their efficacy, and quality control through the manufacturing process all require a different approach, one that encompasses the effects of all factors influencing virulence. Unfortunately, to this day there is no standardized way to report, or even a clear definition of, phage virulence itself.

In epidemiology, a common measurement of virulence is the reproduction number (R_0)—defined as the average number of additional hosts that the virus will spread to after infecting a single host.²⁹ An equivalent measurement is not applicable to the virulent phage life cycle. The number of phage progeny released per infected cell is given by the burst size; when replicating in a healthy densely growing bacterial culture, the R_0 of a phage is essentially equal to its burst size. However, burst size alone is not a proper indicator of phage virulence. For example, in a study of the efficacy of phage therapy, virulence was found to be an increasing function of both adsorption rate and burst size.²⁷

In fact, even more parameters are needed to fully quantify virulence; these include, among others, the latent period, adsorption efficiency, and host cell growth rate.³⁰ In this context, virulence can be defined as the ability of a phage to kill or damage a host population.³¹ As pointed out by Hobbs and Abedon,³² the concept of virulence is often applied to differentiate phages undergoing lytic rather than lysogenic or chronic infections. But even in the case of comparing strictly lytic phages or various clones of a strictly lytic phage, it is possible to infer different degrees of virulence, despite the inconsistencies in terminology.

Common techniques employed to qualitatively measure virulence are spot tests on agar plates³³ and bacterial reduction curves.³⁴ A spot test entails spreading a small sample of a specific phage over a bacterial culture growing in a top-agar lawn. This is a quick way to test susceptibility of a bacterial strain to various phages but does not capture infection dynamics.³⁵ A bacterial reduction curve is obtained by infecting a liquid bacterial culture with phages and taking periodic optical density measurements, which will be reduced compared with those of a phage-free control. A typical virulence study consists of generating bacterial reduction curves under various conditions and qualitatively comparing which bacterial curve is “reduced” the most. The advantage of this approach is that it is applicable to any phage cultivable in suspended cultures. The disadvantages are that it is time consuming, nonstandardized, and only qualitative in its current incarnation. Examples of bacterial reduction curves are plentiful in the literature.^{34,36–44} Although all these experiments rely on the same principle, no standardized or quantitative method has emerged to quantify virulence or facilitate comparisons across conditions and studies.

In one study, four isolated phages specific to *Escherichia coli* O157:H7 were screened against hundreds of *E. coli* strains to gather host range and susceptibility data.⁴⁴ The protocol consisted of performing bacterial infections in 220- μ L volumes using 96-well plates. Bacterial cultures at the same optical density were inoculated with phages at initial multiplicities of infection (MOIs) ranging from 10^{-6} to 10^2 . Plates were incubated at 37°C for 5 h and then visually observed for signs of cell lysis. Host cell susceptibility was then categorized based on the minimum MOI required to obtain culture-wide lysis by visual inspection. This approach offers many improvements over the current mixture of nonstandardized protocols adopted by different researchers. But it has shortcomings. First, it relies on visual inspection rather than a measurable property. Second, it fails to capture the dynamics of infection, instead relying on endpoint measurements, which can be misleading. Third, it defines lytic capability in terms of susceptibility of the host rather than the phage.

Another study evaluated the infectivity of a phage or of a combination of phages by comparing the areas under the curve of optical density for infected and noninfected bacterial cultures.⁴⁵ Recently, Xie et al.⁴⁶ built on this concept to demonstrate how bacterial reduction curves performed in microplates can be used for the high-throughput evaluation of host range and phage infectivity. In the study, the authors demonstrated how the comparison of the areas under the curves could be used to semiquantify the efficacy of a phage against a given host or a range of hosts.

In this study, we detail a method to measure phage virulence that overcomes the shortcomings faced by traditional methods. We build on the premise that comparisons between infected and noninfected bacterial cultures can be used to quantitatively assess the virulence of a phage or phage mixture—as demonstrated in Refs.^{45,46} This method generates a virulence index (V_p) for a phage infecting a specific host strain under a given set of environmental conditions. This study, which compares the virulence of phages T4, T5, and T7 under various conditions, shows the virulence index can be used to easily compare and quantify the virulence of diverse phages. This protocol greatly simplifies and improves the reliability of virulence measurements and provides a platform to quantitatively compare between phages and conditions.

Materials and Methods

Organisms and media

Cultures of *Escherichia coli* ATCC 11303 used for experimentation were grown overnight in 10 mL of medium. The media used were Bacto Tryptic Soy Broth (TSB; Becton Dickinson, Sparks, MD) and BBL Brain Heart Infusion (BHI; Becton Dickinson). Host cultures were grown in 125-mL Erlenmeyer flasks containing 10 mL of medium, agitated at 150 rpm and incubated at 37°C. Phage species used were phage T4 (ATCC 11303-B4), phage T5 (ATCC 11303-B5), and phage T7 (ATCC 11303-B7). Phage stocks were stored at 4°C in TSB at titers of 4.5×10^8 , 2.3×10^8 , and 2.1×10^8 pfu/mL, respectively.

Bacterial reduction experiments

Overnight cultures (100 μ L) were used to inoculate 10 mL of fresh medium in an Erlenmeyer flask, incubated at 37°C and agitated at 150 rpm. These cultures were allowed to grow beyond the starting bacterial concentration used for the bacterial reduction experiments (10^8 cfu/mL). All bacterial reduction curves were generated using 96-well plates with 300- μ L well volumes. Phage stocks were serially diluted from a concentration of 10^8 to 10 pfu/mL in 200- μ L volumes. Plates were incubated at 37°C for 30 min before inoculation to ensure stable temperatures. Cell concentrations were adjusted to 10^8 cfu/mL for every experiment, unless otherwise indicated, yielding MOIs ranging from 10^{-7} to 1. In this report, MOI refers to the initial MOI at the initiation of phage infection. Considering that the working volume used to generate the reduction curves was 250 μ L, MOIs lower than 10^{-7} were not tested, since, on average, they would have less than one phage per culture.

A layout of the microplate used for high-throughput evaluation of virulence is shown in Figure 1A. Five wells of phage-free bacterial cultures were included on every plate as control experiments, in addition to three media blanks for reference. Experiments were run with all phage samples

growing in parallel in a final volume of 250 μL . Since phages are serially diluted to obtain different MOIs, this setup can be completed rapidly with a multichannel pipetter. Optical density was measured at 630 nm with a Bio-Tek ELx800 Universal Microplate Reader and the data were recorded using KCJunior software. It should be noted that other wavelengths could be used (recommended range 500–650 nm) but that it should be kept constant for any single study.

Optical density measurements were taken immediately after inoculation and then at regular intervals afterward. Between samples, the plates were covered and placed in an incubator shaker at 150 rpm at the specified experimental temperature (continuous incubation and readings in an incubating plate reader are also possible, even recommended when available). Measurements were taken until the control cultures reached stationary phase.

Once all data were collected, areas underneath the optical density versus time curves were calculated using the trapezoid rule for each well, from the time of infection to the time corresponding to the onset of stationary phase in the phage-free control.

Evaluation of phage cocktails

The virulence of two combinations of phages T5 and T7 (at proportional T5:T7 ratios of 1:1 and 3:1) was also assessed using the same procedure as already described, with the particularity that the MOI reported was the combined MOI of both phages. For example, when the ratio of 1:1 was tested, 0.5×10^8 pfu/mL of phage T5 and 0.5×10^8 pfu/mL of phage T7 were used to make a total combined titer of 1×10^8 pfu/mL, for an MOI of 1. Similarly, for the 3:1 ratio, 0.75×10^8 pfu/mL of phage T5 and 0.25×10^8 pfu/mL of phage T7 were used for a total combined titer of 1×10^8 pfu/mL.

The use of the combined MOI is important for the assessment of virulence in comparison with results from single phages; this allows the rapid identification of synergistic or inhibitory effects between phages.

In these tests, the microplate layout described in Figure 1A was still used, where triplicates of phage cocktails occupied three columns. Incubation in TSB at 37°C, measurements, and analysis were conducted in the same manner as for single phage testing.

Statistical analysis

Virulence assays for each phage species were performed in duplicate on three separate microwell plates ($n=6$) or in triplicate in a single plate ($n=3$) for the comparison of phage cocktails. This was done so that inaccurate readings or potential contamination could be detected. Data points on graphs are shown as the average of all replicates; error bars depict the standard deviation. Errors reported for virulence index (V_P —defined in the Virulence protocol and nomenclature section below) values are the summation of errors in all the local virulence (v_i —also defined below) values from which V_P was determined.

Results

Virulence protocol and nomenclature

The virulence measurements presented herein build on the premise of bacterial reduction curves. A set of bacterial re-

duction curves—performed as described in the previous section—for T4 infecting *E. coli* ATCC 11303 in TSB at 37°C is shown in Figure 1B. The phage-free control exhibits a classic growth pattern. By comparing the bacterial reduction curves with the control, we can quantify the reduction due to the killing or damaging of the host by the phage. This is done by comparing the integrated area of a bacterial reduction curve (A_i , where i is the MOI) with the integrated area of the phage-free control (A_0) as shown in Figure 1C for the MOI 10^{-3} . These areas are calculated from the onset of infection (time 0) to the time of the onset of the stationary phase in the phage-free control (indicated by the vertical dashed gray line near 3 h in Fig. 1C).

It is important to stress how the establishment of the limit of integration plays a significant role in the assessment of virulence. This limit should be set as the onset of stationary phase in the phage-free control. This provides a consistent reference for integration that can be easily identified for any phage–host system and restricts measurements to the period of cell growth—a necessary condition for productive infection for many phages.⁴⁷ Moreover, it ensures that the range of the virulence measurements is well distributed, as discussed hereunder. In general, we recommend establishing the limit of integration as the time at which the slope of OD_{630} over time reaches ≤ 0.03 h.

Using the two areas calculate for the free-phage control (A_0) and the culture infected at a given MOI (A_i), a local virulence (v_i), capturing the dynamics of phage infection, can be calculated for that specific MOI under a given set of conditions:

$$v_i = 1 - \frac{A_i}{A_0}, \quad (1)$$

where v_i reports the killing or damaging ability of the phage at a given MOI. The more virulent a phage, the faster it kills a large number of bacteria (or prevents them from growing), and the greater v_i . The local virulence is measured on a scale from 0 to 1, where 0 represents the absence of virulence and 1 represents maximum theoretical virulence—instantaneous cell death. Although this theoretical maximum is unlikely to be observed in the laboratory, a $v_i > 0.90$ is readily achievable with the appropriately lytic phage–host system.

In addition, a virulence curve (Fig. 1E) can be obtained for the phage grown under a given set of environmental conditions (e.g., temperature, medium, and ionic strength) by plotting local virulences calculated from Figure 1B against \log MOI (which is easily obtained from the conversion of the MOI axis shown in Fig. 1D). This provides a powerful tool in characterizing a phage against a specific host over a large range of MOIs. In general, the earlier v_i approaches 1 on the virulence curve, the more virulent the phage. Two important values can be gathered from such virulence curves to quantify phage virulence: the virulence index (V_P , where P refers to the phage species) and MV_{50} (MOI required to produce a local virulence of 0.5).

The virulence index is defined as the area under the virulence curve (A_P) divided by the theoretical maximum area under the virulence curve (A_{max}):

$$V_P = \frac{A_P}{A_{max}}, \quad (2)$$

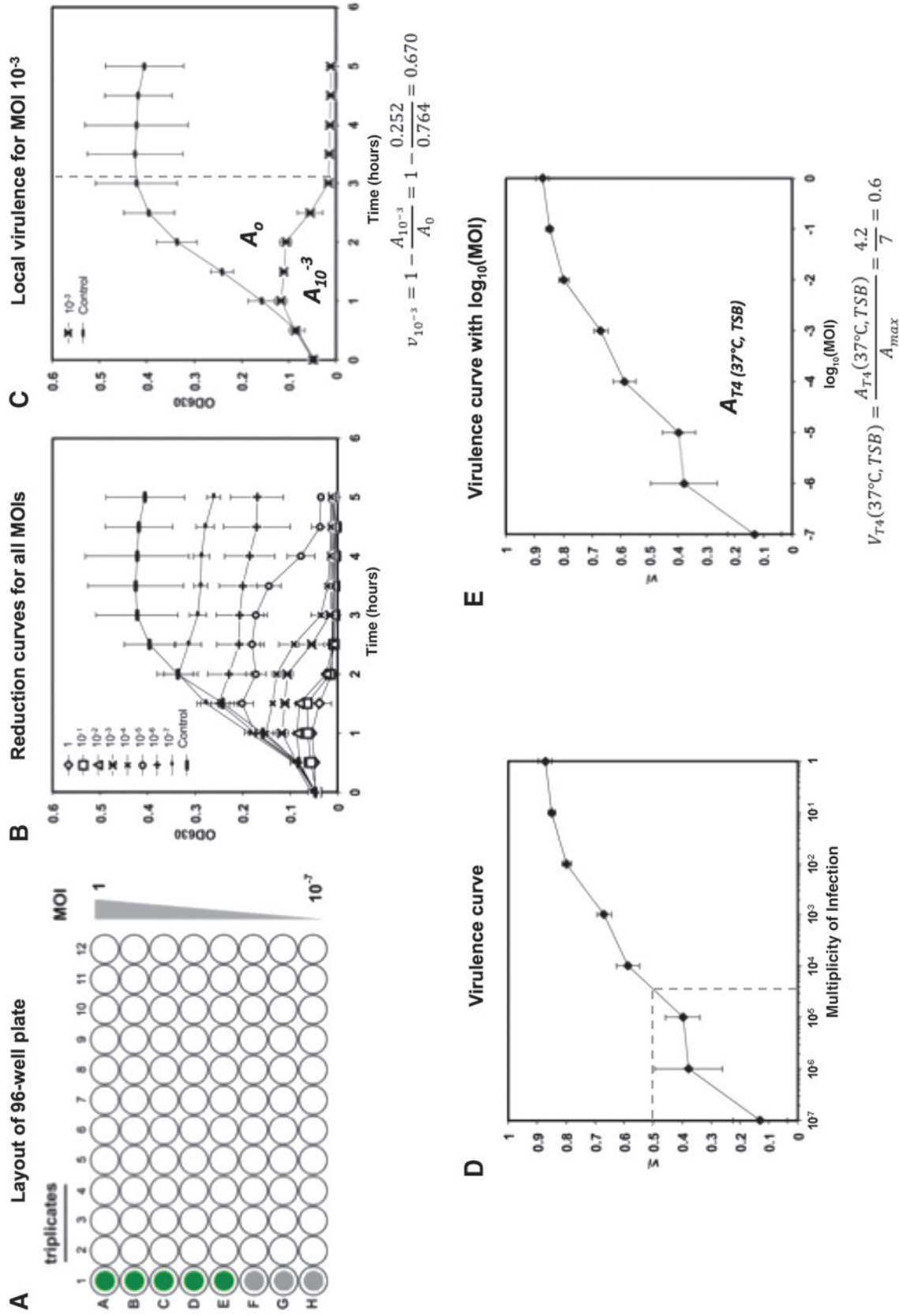


FIG. 1. (A) Layout of 96-well plate for high-throughput evaluation of virulence. Column 1 is used for controls; green wells for phage-free cultures, gray wells for media blanks. Each column is used to test a different phage. Each row indicates a different initial MOI, from 1 (row A) to 10^{-7} (row H). (B) Bacterial reduction curves for phage T4 infecting *Escherichia coli* ATCC 11303 in TSB at 37°C. (C) Obtaining the local virulence (v_i) at a given MOI (example shown for MOI 10^{-3}). Growth curve of phage-free control and bacterial reduction curve at MOI 10^{-3} (extracted from B). The dashed vertical line indicates the limit of integration. The equation for local virulence is shown below the graph and its value is obtained from the areas under the bacterial reduction curve ($A_{10^{-3}}$) and under the growth curve (A_0). (D) Virulence curve generated from bacterial reduction curves of phage T4 growing in TSB at 37°C. Each individual data point represents the local virulence (v_i) at the corresponding MOI. Dotted line highlights MV50 determination. (E) Virulence curve from (D) with x-axis converted to $\log_{10}(\text{MOI})$. The equation for the virulence index is shown below the graph and its value is calculated from the area under the virulence curve [$A_{T4}(37^\circ\text{C}, \text{TSB})$]. Error bars depict the standard deviation of six replicates. MOI, multiplicity of infection; TSB, Tryptic Soy Broth.

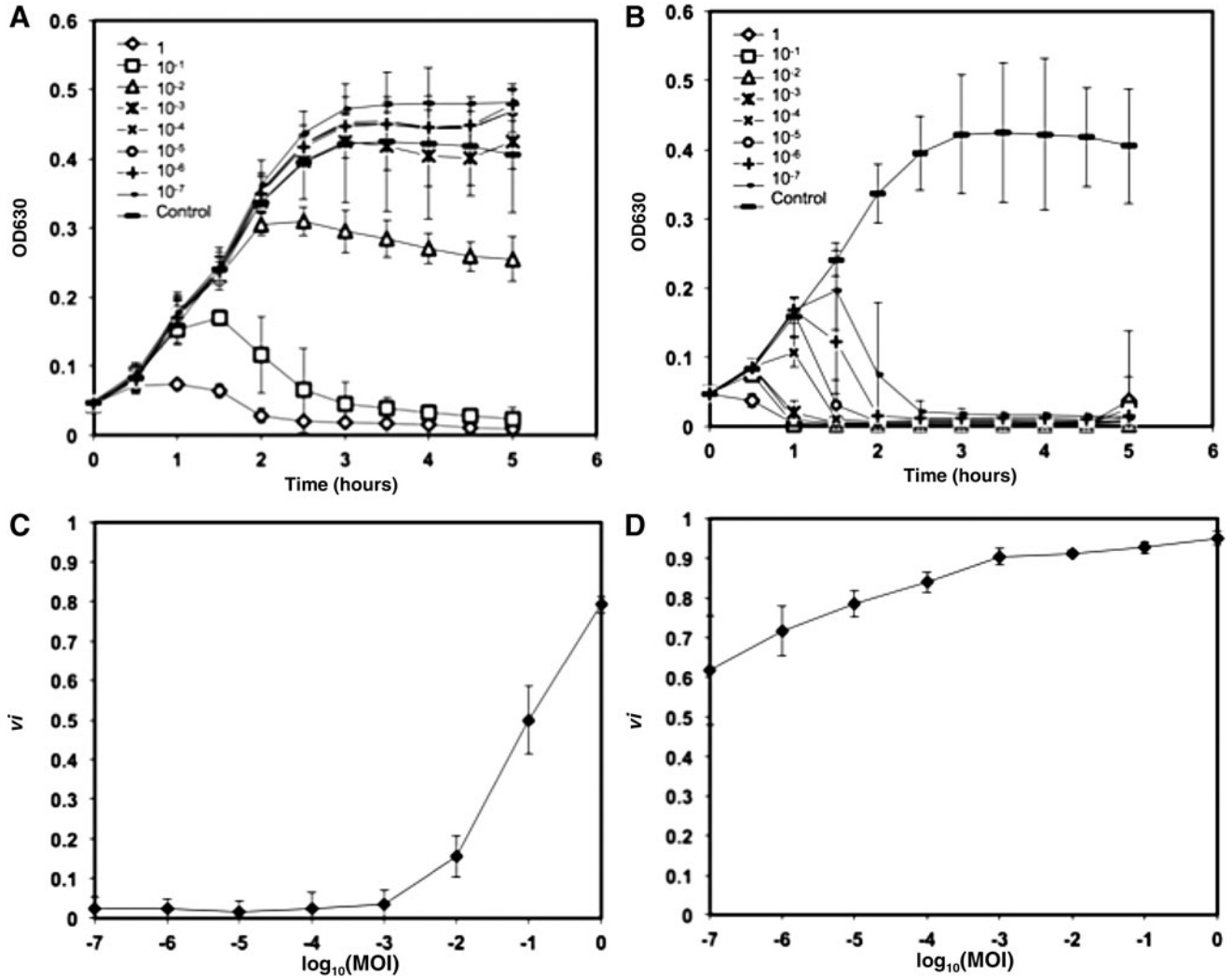


FIG. 2. (A) Bacterial reduction curves and (B) corresponding virulence curve for phage T5 infecting *E. coli* ATCC 11303 in TSB at 37°C. (C) Bacterial reduction curves and (D) corresponding virulence curve for phage T7 infecting *E. coli* ATCC 11303 in TSB at 37°C. Error bars depict the standard deviation of six replicates.

where A_p is determined by integrating the virulence curve according to

$$A_p = \int_{-7}^0 v_i d(\log MOI). \quad (3)$$

Note that $\log MOI$ is used in the integration to give equal weighting to each v_i when calculating the virulence index. The value for A_{max} is determined by Equation (3) under the special condition that $v_i = 1$ for all MOIs. In this study, $A_{max} = 7$ for all conditions tested, since the range of MOIs investigated goes from $\log MOI = -7$ to $\log MOI = 0$.

Similarly to the local virulence, the virulence index is normalized such that the theoretical maximum is 1. To reach this value, instantaneous lysis of the entire bacterial culture for all MOIs tested would be required, a physical impossibility. In this study, the highest virulence index observed was 0.84. A virulence index of 0 signifies the complete absence of virulence over the range of MOIs tested.

From the data shown in Figure 1E (phage T4 in TSB at 37°C), a virulence index of 0.6 was obtained. It was calcu-

lated as follows (integrations calculated using the trapezoid rule):

$$A_{T4}(37^\circ C, TSB) = \int_{-7}^0 v_i d(\log MOI) = 4.2, \quad (4)$$

$$V_{T4}(37^\circ C, TSB) = \frac{A_p}{A_{max}} = \frac{4.2}{7} = 0.6. \quad (5)$$

The final quantitative parameter given by the virulence curve is MV_{50} , an analogue to ID_{50} (infective dose for 50% of subjects) used in toxicology.⁴⁸ It is defined as follows:

$$MV_{50} \equiv MOI|_{v_i=0.5}. \quad (6)$$

MV_{50} is the MOI for which the local virulence v_i is equal to 0.5, the MOI at which the phage achieves 50% of the maximum theoretical virulence; in this case, lower values indicate greater virulence. This provides another tool for comparing phage virulence. MV_{50} can be found through inspection of

the virulence curve. As an example, MV_{50} for phage T4 at 37°C in TSB obtained from Figure 1D is

$$MV_{50}(T4, 37^\circ C, TSB) \equiv MOI|_{v_i=0.5} = 4 \times 10^{-5}. \quad (7)$$

Note that MV_{50} should be reported to only one significant figure due to the intrinsic error in the virulence curve. This parameter is meant as a broad means of comparison of virulence, not as a precise indicator.

Comparison of virulence

Bacterial reduction curves and their corresponding virulence curves are shown for phage T5 (Fig. 2A, B) and phage T7 (Fig. 2C, D) in TSB at 37°C.

Phage T5 was the least virulent phage studied (Fig. 2B). In contrast to the bacterial reduction curves exhibited by phage T4 (Fig. 1D) and phage T7 (Fig. 2D), phage T5 only began to show measurable virulence at MOIs $\geq 10^{-2}$. For all MOIs lower than this threshold, the values of local virulence observed were 0 (Fig. 2A). Although being noticeable only from an MOI of 10^{-2} , the local virulence increased rapidly, peaking at 0.8 at an MOI of 1. Accordingly, the virulence index measured for T5 under the conditions tested was $V_{T5}(37^\circ C, TSB) = 0.17$.

Phage T7 was the most virulent phage tested under these conditions and yielded a virulence index of 0.84 (from Fig. 2D). The remarkably virulent nature of this phage is observed qualitatively in the bacterial reduction curves (Fig. 2C). At MOIs ranging from 1 to 10^{-3} , culture-wide lysis was achieved within 1 h. Even at the lowest MOI tested (10^{-7}), culture-wide lysis was observed after 2.5 h, whereas the phage-free control grew to stationary phase in 3 h (Fig. 2C).

Although the virulence curves can be used to quickly and effectively compare different phages, mutants or progeny, they also provide excellent visual tools for analysis and comparison of how a phage behaves under a set of conditions. For example, Figure 3 compares the virulence curves for phages T4, T5, and T7 in different environmental conditions. It is clear from these curves that temperature (Fig. 3A, B) and media composition (Fig. 3B, C) can, in some cases, significantly impact phage virulence. Importantly, the same range of MOIs must be used when comparing virulence across different phage species or conditions. If virulence measurements were limited to MOIs ranging from 10^{-2} to 1, inspection of Figure 3C would lead one to conclude that phages T4 and T7 have very similar behaviors. However, inspection of the entire experimental range demonstrates significant differences in the virulence between these phages.

Table 1 displays the virulence index (V_p) and MV_{50} values for phages T4, T5, and T7 in two different media (TSB and BHI) at two different temperatures (30°C and 37°C). The data demonstrate the full spectrum of virulence, from the limited virulence of phage T5 in BHI at 37°C ($V_{T5} = 0.05$, $MV_{50} > 1$) to the exceptional virulence of T7 in TSB at 37°C ($V_{T7} = 0.84$, $MV_{50} < 10^{-7}$). Together the virulence index and the MV_{50} values provide a framework for assessing the virulence of a phage and for comparing phage virulence across species and conditions.

Using the values calculated for phages T4, T5, and T7, it is a straightforward task to identify the relative virulence of each phage. Phage T7 had the highest virulence values and lowest MV_{50} values in all conditions tested. Phage T5

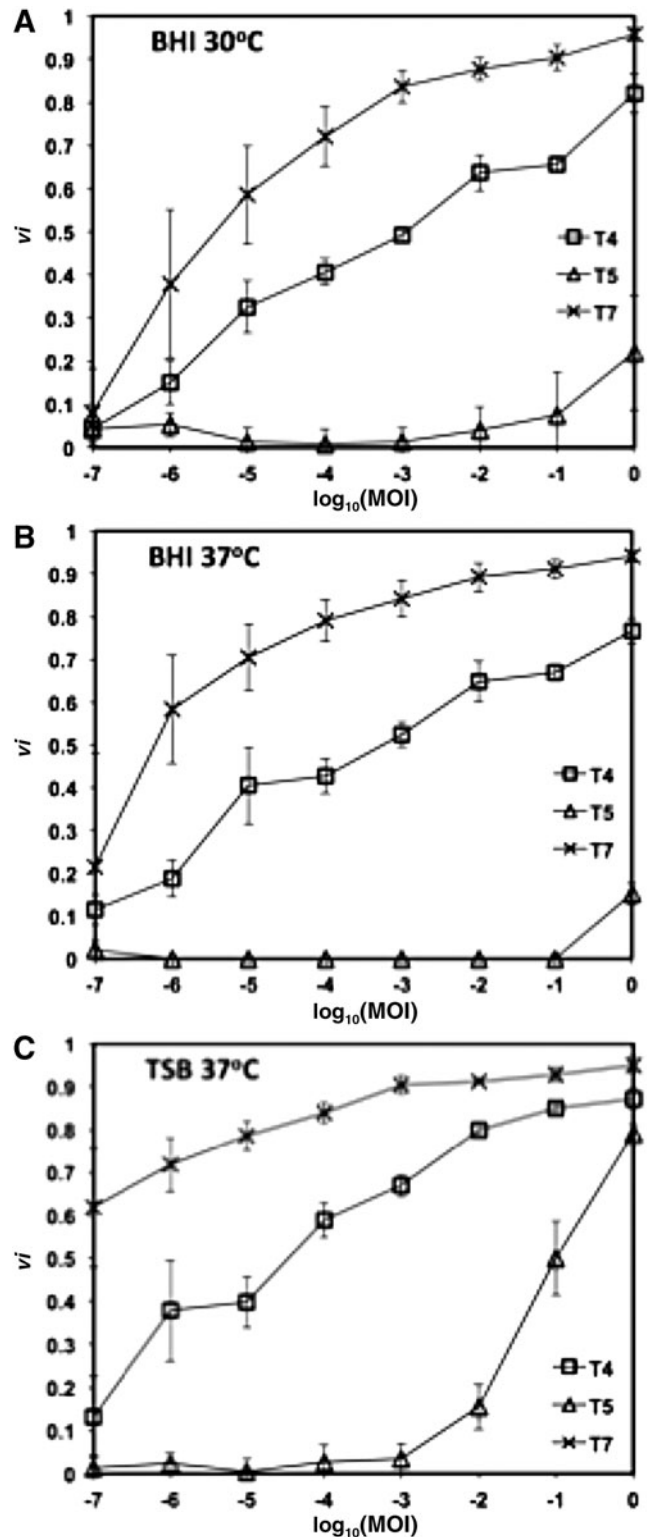


FIG. 3. Virulence curves of phages T4, T5, and T7 in (A) BHI at 30°C, (B) BHI at 37°C, and (C) TSB at 37°C. Error bars depict the standard deviation of six replicates. BHI, Brain Heart Infusion.

TABLE 1. VIRULENCE AND MV_{50} VALUES FOR PHAGES T4, T5, AND T7, AND COMBINATIONS OF PHAGES T5 AND T7 UNDER VARIOUS CONDITIONS

Phage	Virulence index (V_p)				MV_{50}			
	30°C		37°C		30°C		37°C	
	TSB	BHI	TSB	BHI	TSB	BHI	TSB	BHI
T4	0.55 ± 0.07	0.45 ± 0.04	0.60 ± 0.04	0.47 ± 0.05	1 × 10 ⁻⁴	1 × 10 ⁻³	4 × 10 ⁻⁵	6 × 10 ⁻⁴
T5	0.28 ± 0.02	0.05 ± 0.06	0.17 ± 0.05	0.01 ± 0.01	5 × 10 ⁻¹	>1	1 × 10 ⁻¹	> 1
T7	0.77 ± 0.05	0.69 ± 0.08	0.84 ± 0.05	0.76 ± 0.09	8 × 10 ⁻⁷	6 × 10 ⁻⁷	<10 ⁻⁷	4 × 10 ⁻⁶
T5:T7 _(1:1)	—	—	0.81	—	—	—	5 × 10 ⁻⁶	—
T5:T7 _(3:1)	—	—	0.72	—	—	—	1 × 10 ⁻⁶	—

BHI, Brain Heart Infusion; TSB, Tryptic Soy Broth.

consistently had the lowest virulence and highest MV_{50} values. The effect of media conditions on virulence is also apparent. For all phages, BHI unfailingly resulted in lower virulence values. However, the effect of temperature, over the admittedly narrow range tested, was more muted. For phage T4, no significant effect of temperature on virulence was seen between 30°C and 37°C. For T7, virulence increased with temperature, whereas it decreased for T5.

Evaluation of combinations of phages

Similarly, the virulence curves for the mixtures of phages T5 and T7 provide information on the performance of combinations of phages or of phage cocktails. As can be observed in Figure 4, the reduction curves of the combinations of phages (ratios of phages T5–T7 of 1:1 and 3:1) demonstrate a killing potential between those of the single phages, with the 1:1 ratio showing more virulence. This is also observed in the resulting values of virulence index (0.81 and 0.72, respectively) and MV_{50} (5×10^{-6} and 1×10^{-6} , respectively). It is interesting to note that the virulence indexes obtained are not proportional to the relative initial abundance of each phage in the cocktail. This is consistent with the fact that, in the absence of interference or inhibition between them, the contributions of individual phages in a cocktail depend on their individual infection kinetic parameters.

Discussion

As mentioned previously, researchers have been using qualitative observations of bacterial reduction curves to describe phage virulence for many years. In fact, groups have proposed a cell susceptibility scale based on visual observations of the bacterial reduction curve²⁴ and a primary comparison of the area under reduction curves.^{45,46} The virulence index and MV_{50} measurements forego these limitations and enable direct quantitative comparisons of phage virulence, compounding all the parameters affecting it.

The local virulence and virulence index are valuable tools for screening new phage isolates and comparing phages for specific applications. Consider the case of the bacterial reduction curve for phage T7 at an MOI of 10^{-7} (Fig. 2C). It achieved a local virulence value of $v_{10^{-7}} = 0.62$, and complete lysis of the culture occurred within 2 h, astonishingly fast considering such a low MOI. In fact, the virulence curve

(Fig. 2D) begins at this value and increases steadily before stabilizing >0.9 for MOIs $\geq 10^{-3}$. Therefore, for T7, the MV_{50} is $<10^{-7}$. In contrast, for phage T5 under the same conditions, MV_{50} was 10^{-1} —over six orders of magnitude larger than for phage T7. To achieve the same lytic capability as one phage T7, >1 million phage T5 virions are required at the onset of infection.

An important consideration when comparing local virulence, virulence index, and MV_{50} values among various phages and/or conditions is that these parameters are indirect measurements of infection dynamics. Since they are calculated based on the relationship between infected cultures and the growth of the host, they serve as quantitative descriptors of the effect of phages on cell cultures. They are impacted by all the environmental and physiological factors influencing the host and/or phage growth and propagation rates. Thus even if infections may be slower at one set of conditions compared with another (due to slower adsorption rates, longer lysis times, or smaller burst sizes), if the growth of the

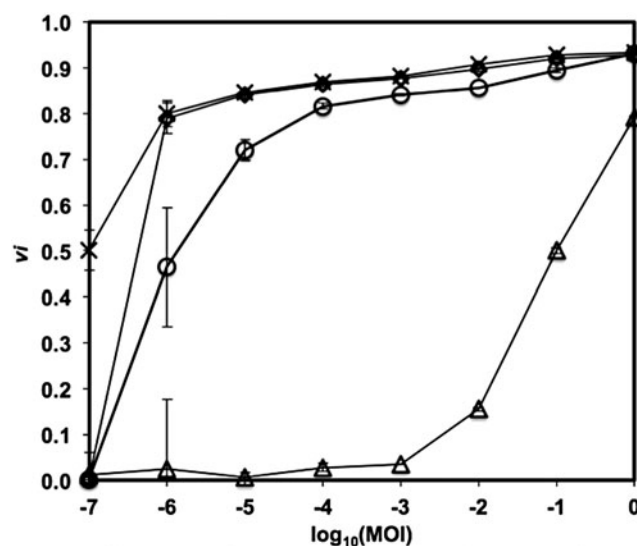


FIG. 4. Virulence curves of phages T5 (triangles), T7 (stars), and combinations of phages T5 and T7 (3:1, circles; 1:1, diamonds) in TSB at 37°C. Error bars depict the standard deviation of triplicates.

host is also slowed down by the same magnitude, the virulence may remain the same. This is a powerful aspect of these measurements: they reflect kinetics without being impeded by them.

Phage virulence is thus affected by a large number of environmental and physiological parameters. For example, conditions such as temperature, pH, media composition, and aeration can all affect both host cell growth rate—influencing phage growth-associated parameters such as burst size and latent period—and phage adsorption rate—affecting the rate of infection.³⁷ Moreover, phage infections at the population level can exhibit characteristics not easily observed in individual host–phage interactions (e.g., lysis inhibition in the case of T4). All these interacting variables contribute to virulence. A recent study testing the efficacy of six newly isolated phages to treat *Pseudomonas aeruginosa* infection of *Drosophila melanogaster* found no correlation between burst size, adsorption rate, or latent period and phage therapy efficacy.²⁸ The only phage parameter found to correlate significantly with treatment efficacy was phage growth rate—implying that a measurement of phage virulence needs to account for contributions of all the disparate factors working together.

With the introduction of the virulence index, there now exists a metric that can be used to quantify the pooled contribution of each of these variables on overall phage virulence. Which features of phages T4, T5, and T7 lead to such significant differences in virulence when infecting *E. coli* in TSB? Phage T4 has a very high adsorption rate and adsorption efficiency in TSB,⁴⁹ whereas T5 and T7 both have similar adsorption rates with poor adsorption efficiencies in the same medium.⁵⁰ Perhaps this poor adsorption efficiency is a major reason why T5 displays limited virulence in TSB. Yet, T7, which has even lower adsorption efficiency, is extremely virulent. In this case, the latent period and/or burst size may be the deciding factors. Although not measured in these experiments, T7 is reported to exhibit latent periods of <20 min and T5's latent period can exceed 40 min.⁵¹ Note that the relative importance of each of these parameters in determining virulence may also be influenced by the bacterial cell density. The virulence curve can be used in conjunction with traditional measurements of phage growth kinetics to determine the contribution each phage growth parameter has on overall phage virulence.

In addition, as highlighted by many studies,^{52–55} the formulation of phage cocktails is crucial to the success of many phage-based treatments and technologies. Considering most cocktails are composed of more than two phages, proper optimization studies require testing vast number of possible formulations, which can be difficult and time consuming. Hence, it would be most practical to perform a large number of comparisons at a given MOI on a single multiplate, essentially comparing the values of local virulence (v_i) for various combinations of phages. In this case, the whole multiplate layout could be modified to have various formulations all at the same MOI (rather than the range of MOIs described and shown in Fig. 1). In contrast, the virulence index and the shape of the virulence curve (Fig. 4) can also be used to further understand some of the interactions between the individual phages making up the cocktail, for example, to see whether the presence of a phage in the cocktail impedes on the overall virulence.

Conclusions

The phage research community and industry require a simple, fast, and standardized way to measure quantitatively phage virulence that takes into account all factors affecting virulence. The methodology developed will facilitate and standardize the important screening steps used in selecting a phage for specific applications. It can serve for the evaluation of mutations or adaptations on virulence. It can also be used to benchmark different phages or production batches for consistency and quality control purposes, or to serve as a reliable comparison platform in the elaboration of formulation of phage cocktails. It can easily be integrated in high-throughput strategies, a non-negligible factor as phage isolation and screening efforts are rapidly expanding. Finally, we hope this method will open new avenues for the assessment and prediction of virulence and efficacy in *in vivo* systems.

Acknowledgments

Funding for this research was provided by the Natural Sciences and Engineering Research Council of Canada, Alberta Innovates Technology Futures, and the University of Alberta Research Experience program. Special thanks to Melissa Harrison who performed the assays for the combinations of T5–T7.

Authorship Confirmation Statement

Z.S. and D.S. designed experiments. Z.S., M.R.T., and K.M. performed experiments and analyzed data. Z.S., M.R.T., and D.S. developed virulence metrics. Z.S., M.R.T., and D.S. wrote the article.

Author Disclosure Statement

No competing financial interests exist.

References

1. Ptashne M. *A Genetic Switch: Phage Lambda Revisited*. Cold Spring Harbor, NY: Cold Spring Harbor Laboratory Press; 2004.
2. Abedon ST; ed. *Bacteriophage Ecology: Population Growth, Evolution, and Impact of Bacterial Viruses*. Cambridge, UK: Cambridge University Press; 2008.
3. Hatfull GF. Innovations in undergraduate science education: Going viral. *J Virol*. 2015;89:8111–8113.
4. Philipson CW, Voegtly LJ, Lueder MR, et al. Characterizing phage genomes for therapeutic applications. *Viruses*. 2018;10:188.
5. Melo LDR, Oliveira H, Santos SB, et al. Phages against infectious diseases. In: Patterson R and Lima N; eds. *Bioprospecting—Success, Potential and Constraints*. Cham, Switzerland: Springer; 2017: 269–294.
6. Merabishvili M, Pirnay JP, Verbeken G, et al. Quality-controlled small-scale production of a well-defined bacteriophage cocktail for use in human clinical trials. *PLoS One*. 2009;4:e4944.
7. Rhoads DD, Wolcott RD, Kuskowski MA, et al. Bacteriophage therapy of venous leg ulcers in humans: Results of a phase I safety trial. *J Wound Care*. 2009;18:237–243.
8. Pirnay JP, De Vos D, Verbeken G, et al. The phage therapy paradigm: Pret-a-porter or sur-mesure? *Pharm Res*. 2011; 28:934–937.

9. Pirnay JP, Verbeken G, Rose T, et al. Introducing yesterday's phage therapy in today's medicine. *Future Virol.* 2012;7:379–390.
10. Jones JB, Jackson LE, Balogh B, et al. Bacteriophages for plant disease control. *Annu Rev Phytopathol.* 2007;45:245–262.
11. Mahony J, McAuliffe O, Ross RP, et al. Bacteriophages as biocontrol agents of food pathogens. *Curr Opin Biotech.* 2011;22:157–163.
12. Lu TK, Collins JJ. Dispersing biofilms with engineered enzymatic bacteriophage. *Proc Natl Acad Sci USA.* 2007;104:11197–11202.
13. Carson L, Gorman SP, Gilmore BF. The use of lytic bacteriophages in the prevention and eradication of biofilms of *Proteus mirabilis* and *Escherichia coli*. *FEMS Immunol Med Mic.* 2010;59:447–455.
14. Huang S, Yang H, Lakshmanan RS, et al. The effect of salt and phage concentrations on the binding sensitivity of magnetoelastic biosensors for *Bacillus anthracis* detection. *Biotechnol Bioeng.* 2008;101:1014–1021.
15. Tawil N, Sacher E, Mandeville R, et al. Surface plasmon resonance detection of *E. coli* and methicillin-resistant *S. aureus* using bacteriophages. *Biosens Bioelectron.* 2012;37:24–29.
16. Singh A, Poshtiban S, Evoy S. Recent advances in bacteriophage based biosensors for food-borne pathogen detection. *Sensors (Basel).* 2013;13:1763–1786.
17. Dang X, Yi H, Ham MH, et al. Virus-templated self-assembled single-walled carbon nanotubes for highly efficient electron collection in photovoltaic devices. *Nat Nanotech.* 2011;6:377–384.
18. Pearson HA, Sahukhal GS, Elasri MO, et al. Phage-bacterium war on polymeric surfaces: Can surface-anchored bacteriophages eliminate microbial infections? *Biomacromolecules.* 2013;14:1257–1261.
19. Josslin R. The lysis mechanism of phage T4: Mutants affecting lysis. *Virology.* 1970;40:719–726.
20. Daniels LL, Wais AC. Virulence in phage populations infecting *Halobacterium cutirubrum*. *FEMS Microbiol Ecol.* 1998;25:129–134.
21. Bronson MJ, Levine M. Virulent mutants of phage P22: II. Physiological analysis of P22 virB-3 and its component mutations. *Virology.* 1972;47:644–655.
22. Storms ZJ, Sauvageau D. Evidence that the heterogeneity of a T4 population is the result of heritable traits. *PLoS One.* 2014;9:e116235.
23. Ceysens P-J, Glonti T, Kropinski AM, et al. Phenotypic and genotypic variations within a single bacteriophage species. *Virol J.* 2011;8:134.
24. Abedon ST. Communication among phages, bacteria, and soil environments. In: Witzany G; ed. *Biocommunication in Soil Microorganisms, Soil Biology Volume 23*. Berlin, Germany: Springer; 2011: 37–65.
25. Maxwell CS. Hypothesis: A plastically-produced phenotype predicts host specialization and can precede subsequent mutations in bacteriophage. *mBio.* 2018;9:e00765-18.
26. Pagliarini S, Korobeinikov A. A mathematical model of marine bacteriophage evolution. *R Soc Open Sci.* 2018;5:171661.
27. Levin BR, Bull JJ. Phage therapy revisited: The population biology of a bacterial infection and its treatment with bacteriophage and antibiotics. *Am Nat.* 1996;147:881–898.
28. Lindberg H, McKean KA, Wang IN. Phage fitness may help predict phage therapy efficacy. *Bacteriophage.* 2014;4:e964081.
29. Dietz K. The estimation of the basic reproduction number for infectious diseases. *Stat Meth Med Res.* 1993;2:23–41.
30. Santos SB, Carvalho C, Azeredo J, et al. Population dynamics of a *Salmonella* lytic phage and its host: Implications of the host bacterial growth rate in modelling. *PLoS One.* 2014;9:e102507.
31. Smith HW, Huggins MB, Shaw KM. The control of experimental *Escherichia coli* diarrhoea in calves by means of bacteriophages. *J Gen Microbiol.* 1987;133:1111–1126.
32. Hobbs Z, Abedon ST. Diversity of phage infection types and associated terminology: The problem with “Lytic or Lysogenic.” *FEMS Microbiol Lett.* 2016;363:fnw047.
33. Kutter E. Phage host range and efficiency of plating. In: Clokie MRJ, Kropinski AM; eds. *Bacteriophages: Methods and Protocols*. New York, NY: Humana Press; 2009:141–149.
34. Niu YD, Johnson RP, Xu Y, et al. Host range and lytic capability of four bacteriophages against bovine and clinical human isolates of Shiga toxin-producing *Escherichia coli* O157:H7. *J Appl Microbiol.* 2009;107:646–656.
35. Kropinski AM, Waddell T, Meng J, et al. The host-range, genomics and proteomics of *Escherichia coli* O157:H7 bacteriophage rV5. *Virol J.* 2013;10:76.
36. Raya RR, Varey P, Oot RA, et al. Isolation and characterization of a new T-even bacteriophage, CEV1, and determination of its potential to reduce *Escherichia coli* O157:H7 levels in sheep. *Appl Environ Microbiol.* 2006;72:6405–6410.
37. Vandersteegen K, Mattheus W, Ceysens PJ, et al. Microbiological and molecular assessment of bacteriophage ISP for the control of *Staphylococcus aureus*. *PLoS One.* 2011;6:e24418.
38. Niu YD, Stanford K, Ackermann HW, et al. Characterization of 4 T1-like lytic bacteriophages that lyse Shiga toxin *Escherichia coli* O157:H7. *Can J Microbiol.* 2012;58:923–927.
39. Niu YD, Stanford K, Kropinski AM, et al. Genomic, proteomic and physiological characterization of a T5-like bacteriophage for control of Shiga toxin-producing *Escherichia coli* O157:H7. *PLoS One.* 2012;7:e34585.
40. Vandersteegen K, Kropinski AM, Nash JH, et al. Romulus and Remus, two phage isolates representing a distinct clade within the Twortlikevirus genus, display suitable properties for phage therapy applications. *J Virol.* 2013;87:3237–3247.
41. Chaudhry WN, Haq IU, Andleeb S, et al. Characterization of a virulent bacteriophage LK1 specific for *Citrobacter freundii* isolated from sewage water. *J Basic Microbiol.* 2014;54:531–541.
42. Niu YD, McAllister TA, Nash JH, et al. Four *Escherichia coli* O157:H7 phages: A new bacteriophage genus and taxonomic classification of T1-like phages. *PLoS One.* 2014;9:e100426.
43. Sausseureau E, Vachier I, Chiron R, et al. Effectiveness of bacteriophages in the sputum of cystic fibrosis patients. *Clin Microbiol Infect.* 2014;20:O983–O990.
44. Wong CL, Sieo CC, Tan WS, et al. Evaluation of a lytic bacteriophage, Phi st1, for biocontrol of *Salmonella enterica* serovar Typhimurium in chickens. *Int J Food Microbiol.* 2014;172:92–101.
45. Bertozzi Silva J, Sauvageau D. Bacteriophages as antimicrobial agents against bacterial contaminants in yeast fermentation processes. *Biotech Biofuels.* 2014;7:123.

46. Xie Y, Wahab L, Gill JJ. Development and validation of a microtiter plate-based assay for determination of bacteriophage host range and virulence. *Viruses*. 2018;10:189.
47. Adams MH. *Bacteriophages*. New York, NY: Interscience Publishers; 1959.
48. Kato T, Kurashige S, Chabbert YA, et al. Determination of the ID50 values of antibacterial agents in agar. *J Antibiot*. 1978;31:1299–1303.
49. Storms ZJ, Arsenault E, Sauvageau D, et al. Bacteriophage adsorption efficiency and its effect on amplification. *Bioproc Biosys Eng*. 2010;33:823–831.
50. Storms ZJ, Smith L, Sauvageau D, et al. Modeling bacteriophage attachment using adsorption efficiency. *Biochem Eng J*. 2012;64:22–29.
51. Foster RA, Johnson FH. Influence of urethane and of hydrostatic pressure on the growth of bacteriophages T2, T5, T6, and T7. *J Gen Physiol*. 1951;34:529–550.
52. Mendes JJ, Leandro C, Mottola C, et al. *In vitro* design of a novel lytic bacteriophage cocktail with therapeutic potential against organisms causing diabetic foot infections. *J Med Microbiol*. 2014;63:1055–1065.
53. Malik DJ, Sokolov IJ, Vinner GK, et al. Formulation, stabilization and encapsulation of bacteriophage for phage therapy. *Adv Coll Interf Sci*. 2017;249:100–133.
54. Forti F, Roach DR, Cafora M, et al. Design of a broad-range bacteriophage cocktail that reduces *Pseudomonas aeruginosa* biofilms and treats acute infections in two animal models. *Antimicrob Agents Chemother*. 2018;62:e02573-17.
55. Cooper CJ, Koonjan S, Nilsson AS. Enhancing whole phage therapy and their derived antimicrobial enzymes through complex formulation. *Pharmaceuticals*. 2018;11:34.

Address correspondence to:

Dominic Sauvageau, PhD

Department of Chemical and Materials Engineering

University of Alberta

9211-116 Street NW

Edmonton, AB T6G 1H9

Canada

Email: dominic.sauvageau@ualberta.ca